JCB Article

Sec6/8 complexes on trans-Golgi network and plasma membrane regulate late stages of exocytosis in mammalian cells

Charles Yeaman, Kent K. Grindstaff, Jessica R. Wright, and W. James Nelson

Department of Molecular and Cellular Physiology, Beckman Center for Molecular and Genetic Medicine, Stanford University School of Medicine, Stanford, CA 94305

Sec6/8 complex regulates delivery of exocytic vesicles to plasma membrane docking sites, but how it is recruited to specific sites in the exocytic pathway is poorly understood. We identified an Sec6/8 complex on trans-Golgi network (TGN) and plasma membrane in normal rat kidney (NRK) cells that formed either fibroblast- (NRK-49F) or epithelial-like (NRK-52E) intercellular junctions. At both TGN and plasma membrane, Sec6/8 complex colocalizes with exocytic cargo protein, vesicular stomatitis virus G protein (VSVG)-tsO45. Newly synthesized Sec6/8 complex is simultaneously recruited from the cytosol to both sites. However, brefeldin A treatment inhibits recruitment to the plasma membrane and other treatments that block exocytosis (e.g., expression of kinase-inactive protein kinase D and low temperature incubation) cause accumulation of Sec6/8 on the TGN, indicating that steady-state distribution of Sec6/8 complex depends on continuous exocytic vesicle trafficking. Addition of antibodies specific for TGN- or plasma membrane–bound Sec6/8 complexes to semiintact NRK cells results in cargo accumulation in a perinuclear region or near the plasma membrane, respectively. These results indicate that Sec6/8 complex is required for several steps in exocytic transport of vesicles between TGN and plasma membrane.

Introduction

In response to external stimuli, many eukaryotic cells develop polarity by reorganizing the plasma membrane into structurally and functionally distinct subdomains (Drubin and Nelson, 1996). Lateral membrane formation in polarizing epithelial cells provides a simple paradigm for how a specialized membrane domain develops (for review see Yeaman et al., 1999). In these cells, lateral membrane formation is initiated by the external spatial cue of E-cadherin–mediated cell–cell adhesion. Reinforcement of lateral membrane identity is achieved, in part, by segregation of post-TGN exocytic and endocytic pathways (for review see Mellman, 1996), and selective interactions of some proteins (e.g., Na/K-ATPase) with membrane cytoskeletal scaffolds (Nelson and Veshnock, 1987); content mixing between lateral and apical membranes is prevented by formation of the tight junction (Cereijido et al., 1998). Concurrently, the surface area of the lateral membrane expands approximately sixfold in the first few hours following initiation of cadherin-mediated cell–cell adhesion (Vega-Salas et al., 1987).

Molecular mechanisms that establish polarized membrane growth domains are being identified. Exocytosis involves SNARE-mediated protein–protein interactions between transport vesicles and plasma membranes (for review see Jahn and Südhof, 1999). In polarized epithelial cells, evidence that t-SNAREs are localized to different plasma membrane domains has been presented (Gaisano et al., 1996; Low et al., 1996; Delgrossi et al., 1997; Fujita et al., 1998), and it is likely that different SNAREs are involved in exocytosis to apical and basal-lateral membrane domains (Ikonen et al., 1995; Low et al., 1998). However, during directed membrane growth in budding yeast and developing neurons there is no spatial correlation between the distribution of t-SNAREs and sites of exocytosis (Brennwald et al., 1994; Garcia et al., 1995). Therefore, it seems that t-SNAREs are

Address correspondence to W. James Nelson, Department of Molecular and Cellular Physiology, Beckman Center for Molecular and Genetic Medicine, Stanford University School of Medicine, Stanford, CA 94305-5345. Tel.: (650) 725-7596. Fax: (650) 498-5286. E-mail: wjnelson@stanford.edu

Charles Yeaman's present address is Department of Anatomy and Cell Biology, University of Iowa, Iowa City, IA 52242.

Kent Grindstaff's present address is Xenoport, Inc., Department of Discovery Biology, 2631 Hanover St., Palo Alto, CA 94304.

Jessica Wright's present address is Department of Biological Sciences, Stanford University, Stanford, CA 94305.

Key words: cell polarity; Golgi apparatus/secretion; cell membrane/metabolism; intercellular junctions/physiology; intracellular membranes/metabolism

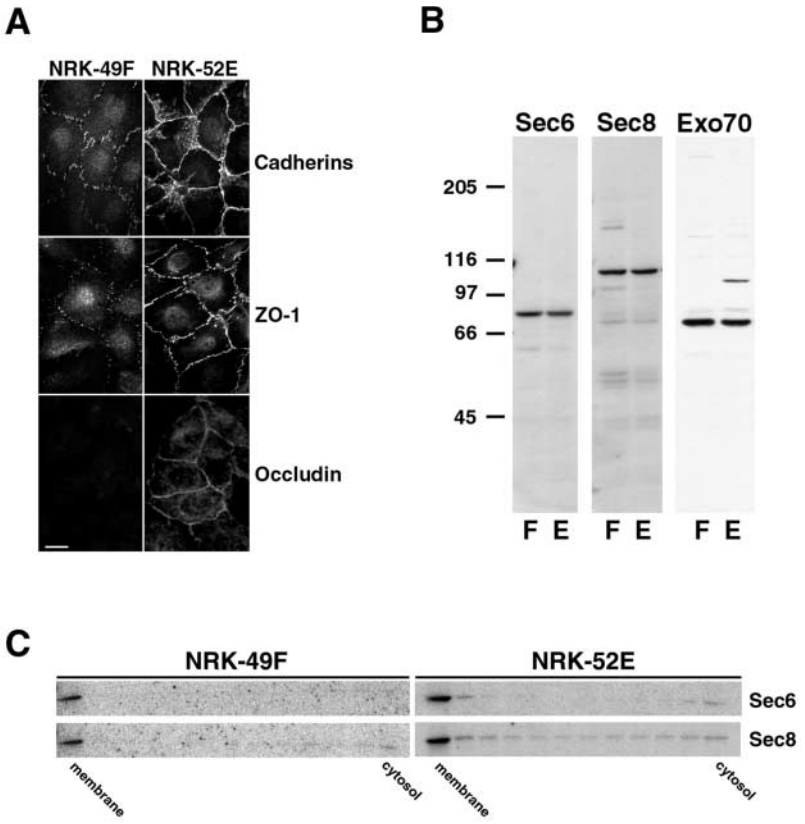

Figure 1. **Sec6/8 complex is associated with membranes in fibroblastic and epithelial-like NRK cells.** (A) Immunofluorescent staining of NRK-49F and NRK-52E cells with antibodies to E/P-cadherin, ZO-1, or occludin. Cells were fixed with 4% paraformaldehyde then extracted with 1% Triton X-100. (B) Immunodetection of Sec6, Sec8, and Exo70 in detergent lysates (50 μg/lane) from NRK-49F (F) and NRK-52E (E) cells. Protein standards indicated are myosin (205 kD), β-galactosidase (116 kD), phosphorylase b (97 kD), bovine serum albumin (66 kD), and egg albumin (45 kD). (C) Separation of membrane-bound and cytosolic Sec6/8 complexes from NRK-49F and NRK-52E cells in 30% (wt/vol) iodixanol gradients. Bar, 20 μm.

necessary but not sufficient for formation of membrane growth domains.

The first component of the exocytic machinery identified at sites of polarized membrane insertion was the Sec6/8 complex (or "exocyst," in yeast) (TerBush and Novick, 1995), an ~750-kD complex consisting of eight subunits (Sec3, Sec5, Sec6, Sec8, Sec10, Sec15, Exo70, and Exo84) (Hsu et al., 1996; TerBush et al., 1996). The Sec6/8 complex is spatially associated with polarized membrane growth areas in budding yeast (TerBush and Novick, 1995), outgrowth areas in neurons (Hazuka et al., 1999), and growing lateral membranes in epithelial cells (Grindstaff et al., 1998). In MDCK cells, introduction of function-blocking Sec8 antibodies into permeabilized cells blocked targeted delivery of a lateral, but not an apical membrane protein (Grindstaff et al., 1998). Furthermore, overexpression of mutant Sec10 protein lacking its COOH terminus inhibited NGF-induced membrane outgrowth in PC12 cells (Vega and Hsu, 2001). In budding yeast, mutations that result in disorganization of the exocyst complex inhibit polarized membrane insertion (Novick et al., 1981). Thus, as in budding yeast, the mammalian Sec6/8 complex is likely to be an essential spatial determinant for polarized membrane growth.

To examine how Sec6/8 complex distribution and function in membrane growth are regulated, we compared two cell types that differ in their organization of intercellular junctions, and by extension, their requirement for polarized membrane growth. We report that Sec6/8 complex is present on both TGN and plasma membranes in nonpolarized fibroblasts and epithelioid cells, but that the relative proportion on these membranes is dependent on both active exocytosis and the complexity of intercellular junctions. We report that Sec6/8 is involved in several steps in exocytosis between TGN and plasma membrane.

Results

Sec6/8 complex localizes to cadherin-based plasma membrane contact sites in fibroblastic and epithelioid NRK cells

Western blot analysis of detergent extracts of fibroblastic normal rat kidney (NRK)*-49F and epithelioid NRK-52E cells (Fig. 1 A) revealed that Sec6, Sec8, and Exo70 are expressed at similar levels in both cell lines (Fig. 1 B) and that most of the Sec6/8 complex was recovered in low-density membrane fractions at the top of iodixanol gradients (Fig. 1 C). Immunofluorescence microscopy of NRK-49F cells fixed before extraction revealed Sec6 staining diffusely distributed throughout the cell, but discontinuous dot-like concentrations of staining were observed along the edges of the plasma membrane between contacting cells (Fig. 2 A). The Sec6-positive dots at the cell periphery were also stained by antibodies to ZO-1, and decorated the ends of parallel bundles of actin filaments stained with rhodamine-phalloidin (Fig. 2 A). In cells that were extracted before fixation, detergent-insoluble protein was localized to spots at membranes between adjacent cells (Fig. 2 A). Bundles of actin filaments appear to terminate in these spots. Note that P-cad-

*Abbreviations used in this paper: BFA, brefeldin A; GFP, green fluorescent protein; NRK, normal rat kidney; ts, temperature sensitive; VSVG, vesicular stomatitis virus G protein.

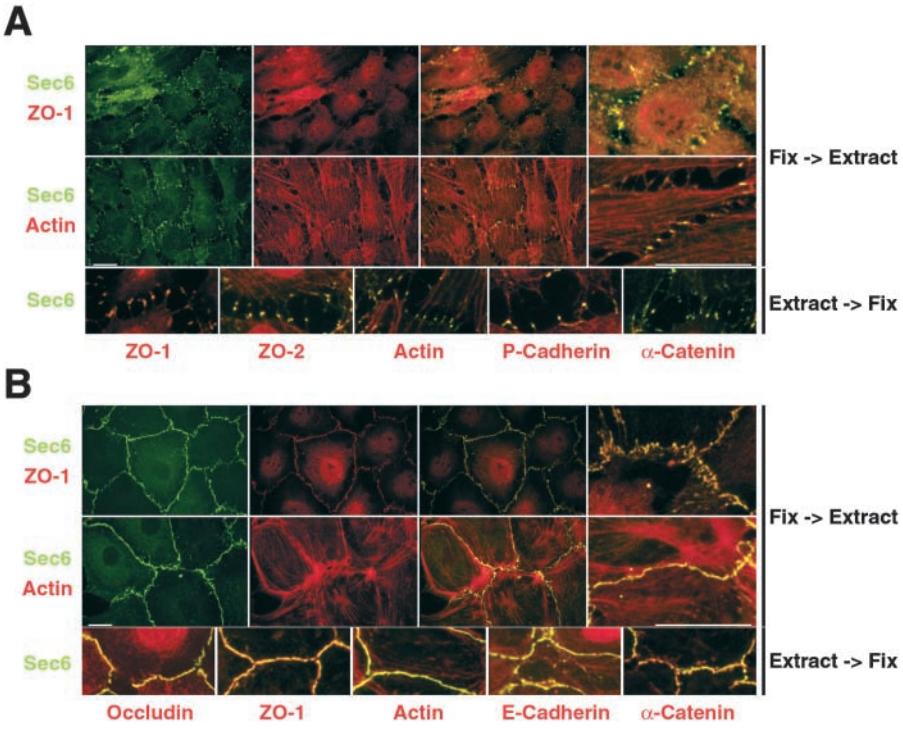

Figure 2. **Sec6/8 complex colocalizes with adhesion junction proteins and actin filaments at cell–cell contact sites in NRK-49F and NRK-52E cells.** NRK-49F cells (A) or NRK-52E cells (B) were fixed with 4% paraformaldehyde before or after extraction with 1% Triton X-100, as indicated. Sec6 (green) distribution was compared with that of ZO-1, ZO-2, occludin, E- or P-cadherin, α-catenin, and filamentous actin (red). Top right of A and B, as well as bottom of A and B show magnified views of cell–cell contacts. Bars, 20 μm.

herin, α-catenin, ZO-1, and ZO-2 coaccumulated in these Sec6-positive spots (Fig. 2 A).

In NRK-52E cells, Sec6 staining was concentrated at the cell periphery in a circumferential ring around each cell that was similar to that of ZO-1 distribution (Fig. 2 B). Actin in NRK-52E cells comprised a cortical belt in addition to stress fibers (Fig. 2 B). Plasma membrane Sec6 staining coincided with cortical actin staining within the boundary of contacting membranes, but was absent from membranes outside the area of cell–cell contact. In cells that were extracted before fixation, Sec6 staining was confined to contacting membranes between cells, where it colocalized with E-cadherin/α-catenin and occludin/ZO-1 (Fig. 2 B). Sec8 staining was indistinguishable from that of Sec6 (unpublished data).

Sec6/8 complex is primarily associated with the TGN in NRK-49F cells

To identify all membrane-associated pools of Sec6/8 complex in fibroblasts, cells were fractionated by isopycnic centrifugation through linear iodixanol gradients. Sec6, Sec8, and Exo70 from NRK-49F cells were recovered in four distinct peaks, with buoyant densities of ~1.04, 1.10, 1.14, and 1.20 g/ml, respectively (Fig. 3 A). A fourth subunit of Sec6/8 complex, Sec5, was also recovered in the same four peaks (unpublished data). The Sec6/8 complex peak recovered at 1.20 g/ml constitutes a relatively minor fraction of the total Sec6/8 complex (~10–20%). Since this peak does not cofractionate with any membrane protein markers, we conclude that it most likely represents a cytosolic pool.

Two plasma membrane proteins, P-cadherin and syntaxin4, were largely (65% and 71%, respectively) recovered near the top of the gradient, indicating that the peak of Sec6/8 complex with a density of 1.04 g/ml represents plasma membrane (Fig. 3 A). Approximately 25% of P-cadherin and syntaxin4 cofractionated with Sec6/8 complex in the peak at 1.14 g/ml. However, attempts to label this fraction of P-cadherin by cell surface biotinylation failed (unpublished data), indicating that this pool is probably in an internal membrane of the exocytic or endocytic pathway. Indeed, marker proteins of the TGN (VAMP4) and early/recycling endosomes (syntaxin13) were broadly distributed across a density range of ~1.08–1.16 g/ml, which overlapped with Sec6/8 complex peaks at 1.10 and 1.14 g/ml (Fig. 3 A). Endoplasmic reticulum (BiP), mitochondria (mtHSP70), and late endosome/lysosome (VAMP7) were recovered in fractions of slightly higher density (~1.18 g/ml), and thus had distributions different from those observed for Sec6/8 complex (unpublished data). The amount of Sec6/8 complex in the peak at 1.10 g/ml varied between experiments. We conclude that in NRK-49F cells, 20–30% of Sec6/8 complex is associated with plasma membrane, and the majority (60–70%) is associated with either TGN or early/recycling endosomes. Note that at least four subunits (Sec5, Sec6, Sec8, and Exo70) are shared between Sec6/8 complexes on different membranes, though subunit stoichiometries of these different complexes may not be the same.

Fractionation of NRK-52E cells in iodixanol gradients revealed a relatively simple distribution of Sec6/8 complex compared with that in NRK-49F cells (Fig. 3 B). The majority of Sec6/8 complex (70–75%) was recovered in a single peak with a density of ~1.04 g/ml. Since this peak cofractionates with the most abundant pool of E-cadherin (45%) and has the same density as that of plasma membrane from NRK-49F cells, we conclude that most of Sec6/8 complex in NRK-52E cells is bound to plasma membrane. In contrast to NRK-49F cells, only a relatively minor amount of Sec6/8 complex (~20–25%) was recovered in fractions in the density range 1.08–1.16 g/ml that contain the majority of VAMP4.

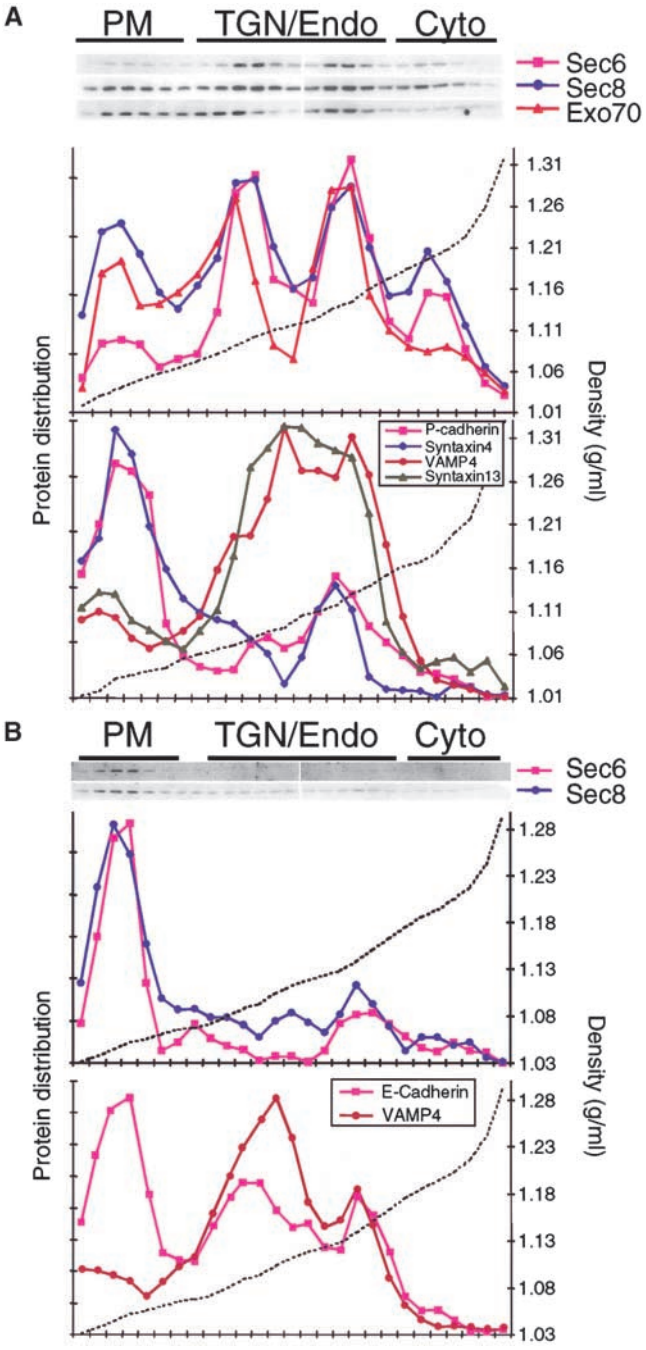

Figure 3. **Fractionation of NRK-49F and NRK-52E cells in iodixanol gradients.** Separation of Sec6, Sec8, Exo70, E- or P-cadherin, VAMP4, syntaxin4, and syntaxin13 from NRK-49F (A) or NRK-52E (B) cell homogenates in 10, 20, and 30% step-iodixanol gradients. PM represents fractions containing the major peak of plasma membrane proteins (E- or P-cadherin, syntaxin4), TGN/Endo represents fractions containing the major peaks of TGN (VAMP4) and early/recycling endosomes (syntaxin13), and Cyto represents fractions that did not contain any membrane protein marker.

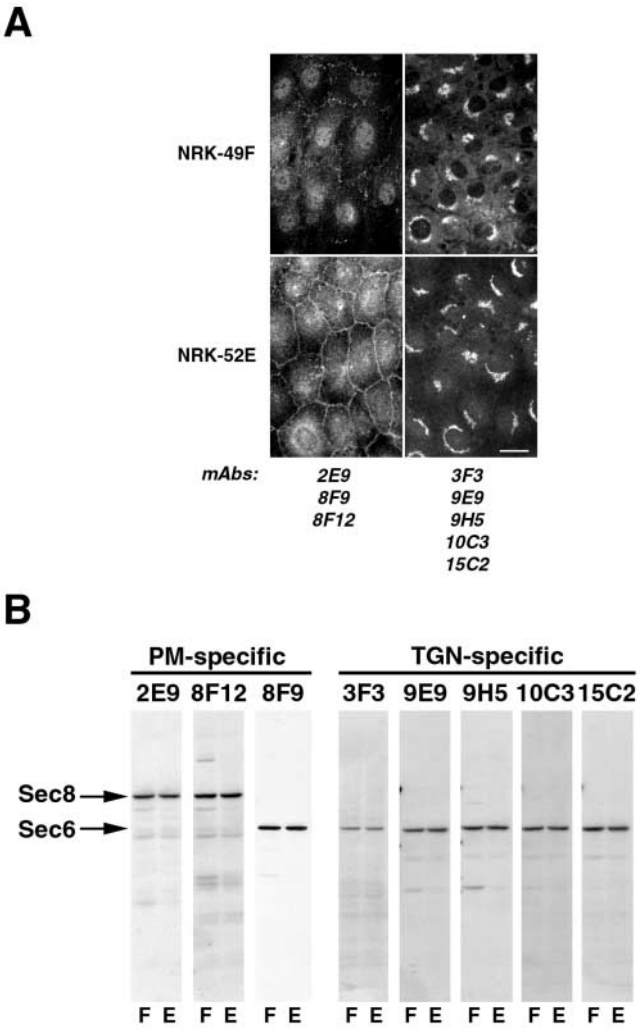

Figure 4. **Sec6/8 complex epitopes are differentially accessible at plasma membrane cell–cell contacts and TGN/endosomes.** (A) NRK-49F and NRK-52E cells were fixed with 4% paraformaldehyde then permeabilized with 0.075% saponin. Left panels show cells stained with anti-Sec8 mAb 2E9, which recognizes Sec8 bound to plasma membrane cell–cell contacts. Right panels show cells that were stained with anti-Sec6 mAb 10C3, which recognizes Sec6 bound to TGN/endosomes. Staining observed with other anti-Sec6 mAbs (3F3, 9E9, 9H5, and 15C2) was identical to that with mAb 10C3. (B) Detection of Sec6 and 8 in detergent extracts (50 μg/lane) of NRK-49F (F) and NRK-52E (E) with different monoclonal antibodies. Bar, 20 μm.

There is significant disparity between the spatial distribution of Sec6/8 complex (Fig. 2 A) and cell fractionation data demonstrating association of Sec6/8 complex with TGN/endosome membranes in NRK-49F cells (Fig. 3 A). It is possible that Sec6/8 complex epitopes are exposed at plasma membrane cell–cell contacts, but masked when the Sec6/8 complex is bound to TGN/endosomes. To address this possibility, we analyzed a panel of monoclonal antibodies to Sec6 and Sec8. This screen revealed antibodies (mAbs 2E9, 8F9, and 8F12) that stained Sec6/8 complex at plasma membrane cell–cell contact sites, and other antibodies (mAbs 3F3, 9E9, 9H5, 10C3, and 15C2) that stained Sec6/8 complex in a perinuclear compartment (Fig. 4 A). These staining patterns were mutually exclusive. To verify that the observed staining was specific for Sec6 and Sec8, each monoclonal antibody was tested by immunoblotting detergent extracts of NRK cells (Fig. 4 B).

Since TGN, early endosomes, and recycling endosomes are not resolved from each other in isopycnic iodixanol gradients (Fig. 3 A), cells were costained with antibodies against

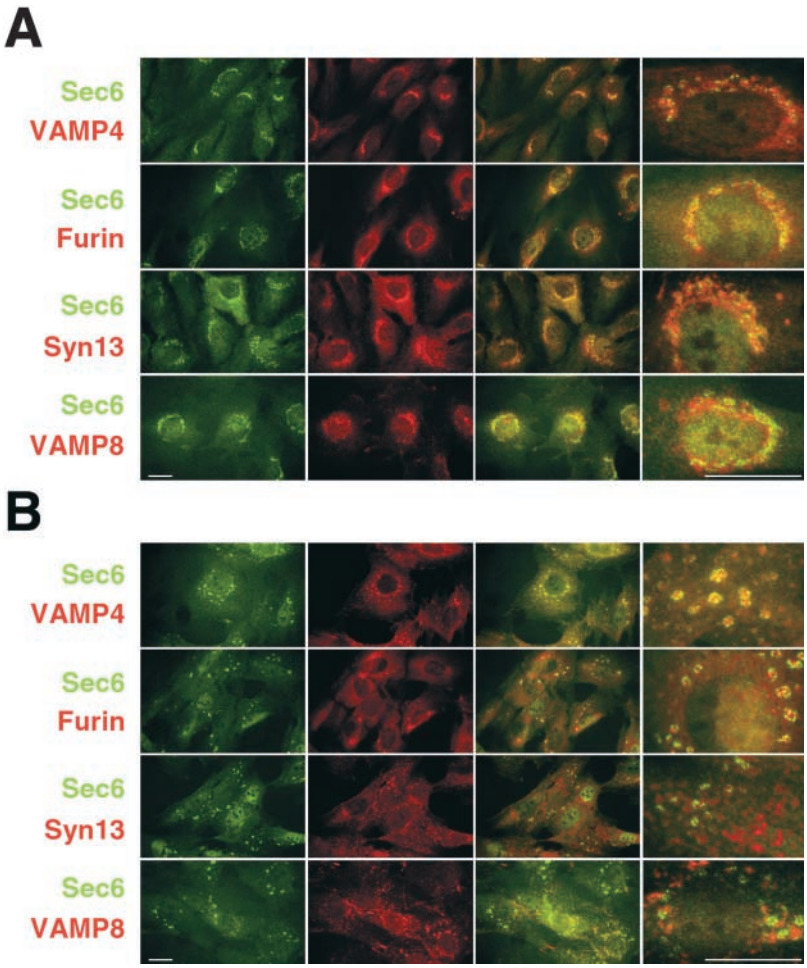

Figure 5. **Immunofluorescent staining of Sec6 and TGN/endosome markers in cells treated with and without nocodazole.** NRK-49F cells were cultured in the absence (A) or presence (B) of 20 μg/ml nocodazole for 2 h. Cells were fixed with 4% paraformaldehyde, then permeabilized with 0.075% saponin. Sec6 staining (mAb 9E9) was compared with that of VAMP4, furin, syntaxin13, or VAMP8. Far right panels in each row of images show magnified views of perinuclear membranes from individual cells. Bars, 20 μm.

Sec6 and either VAMP4 or furin (TGN; Molloy et al., 1994; Steegmaier et al., 1999), VAMP8 (early endosome; Wong et al., 1998), or syntaxin13 (early/recycling endosomes; Prekeris et al., 1998) to determine which of these compartments contained Sec6/8 complex. Each of these antibodies stained perinuclear vesicular structures that partially or entirely surrounded the nucleus (Fig. 5 A). Furin, syntaxin13, and VAMP8 also localized to more peripheral membranes, which likely represent early endosomes. Sec6 was not detected on these peripheral membranes, but was confined to membranes in the perinuclear region. Careful inspection of the perinuclear region reveals that Sec6 staining more closely colocalized with VAMP4 and furin than either syntaxin13 or VAMP8 (Fig. 5 A, magnified views). However, this colocalization was not always precise. Frequently, Sec6-positive vesicular elements appeared to be slightly offset from VAMP4- or furin-positive membranes, and in some instances appeared as a ringlet surrounding a VAMP4- or furin-positive structure.

We examined Sec6 distribution in cells treated with the microtubule-depolymerizing drug nocodazole which induces fragmentation of both TGN and endosomal membranes. Sec6 staining in nocodazole-treated cells was concentrated on membrane fragments that were scattered throughout the perinuclear region in a distribution that was more similar to that of VAMP4 and furin than those of syntaxin13 or VAMP8 (Fig. 5 B). As in control cells (see above and Fig. 5 A), there were subtle differences between Sec6 and VAMP4/furin distributions (Fig. 5 B, magnified views).

Additional evidence that Sec6/8 complex is primarily associated with TGN and not endosomes was obtained by determining whether Sec6-positive compartments were accessible to endocytic (Texas red transferrin; Fig. 6 A) or exocytic (green fluorescent protein [GFP]–vesicular stomatitis virus G protein [VSVG] protein; Fig. 6 B) cargo. Internalization of Texas red transferrin for 5 min labeled a population of vesicular structures in the cell periphery that were negative for Sec6 (Fig. 6 A). Following a 30 min (or 60 min; unpublished data) uptake, transferrin labeled a perinuclear tubulovesicular compartment that was in the same general vicinity as membranes containing Sec6/8 complex. However, there was no overlap in the distributions of Sec6 and transferrin.

To determine whether Sec6/8-containing membranes were accessible to exocytic cargo, cells were transiently transfected with plasmid encoding a GFP-tagged form of the temperature-sensitive (ts) envelope glycoprotein of vesicular stomatitis virus (ts-G-GFP) (Scales et al., 1997). At 40°C, ts-G-GFP fails to fold correctly and accumulates in the ER in a distribution similar to that of the ER-resident protein BiP (Fig. 6 B). No overlap between ER-localized ts-G-GFP and Sec6 is evident, consistent with results that Sec6 does not cofractionate with ER markers in density gradients (Fig. 3). Upon shifting cells to 19°C, a bolus of ts-G-GFP folds and exits the ER, but is subsequently arrested in the TGN.

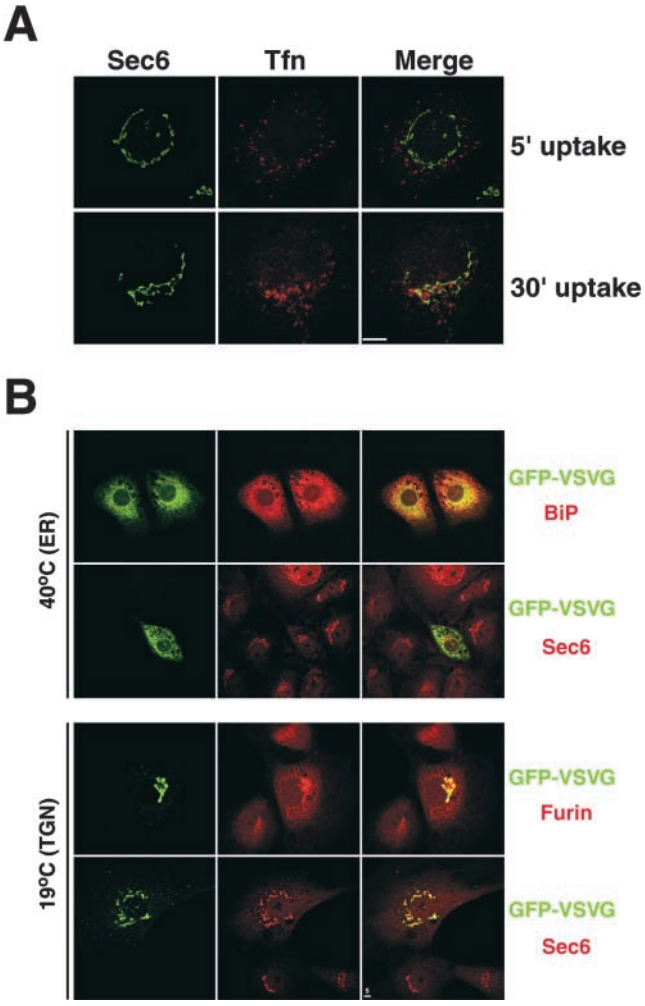

Figure 6. **Immunofluorescent staining of Sec6 compared with endocytic and exocytic cargo.** (A) NRK-49F cells were labeled with Texas red transferrin as described in Materials and methods. Following internalization for 5 or 30 min, cells were fixed, permeabilized, and stained for Sec6 (mAb 9H5). (B) NRK-49F cells were transiently transfected with plasmid encoding ts-G-GFP, and incubated under conditions to arrest this protein in either the ER or TGN, as described in Materials and methods. Cells were then fixed, permeabilized, and stained for Sec6 (mAb 9H5). Bars, (A) 8 μm; (B) 5 μm.

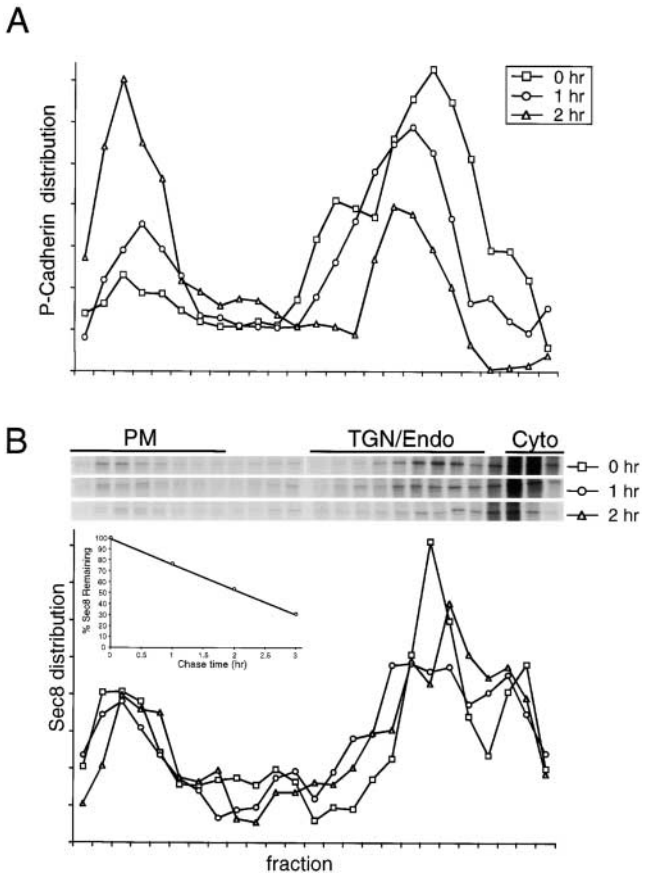

Figure 7. **Metabolic pulse-chase analysis of P-cadherin and Sec8 in NRK-49F cells.** ^{35}S-methionine/cysteine distribution of ^{35}S-methionine/cysteine–labeled P-cadherin (A) and Sec8 (B) in 10–20–30% step iodixanol gradients at different chase times. Plots are normalized to scale of 0 h time point. PM, TGN/Endo, and Cyto were defined as described in the legend to Fig. 3.

At 19°C the distribution of ts-G-GFP is similar to that of furin, though the overlap is not precise (Fig. 6 B). In contrast, ts-G-GFP distribution in cells incubated at 19°C almost perfectly coincides with Sec6 staining (Fig. 6 B). Therefore, Sec6/8 complex appears to be associated with a subcompartment of the TGN that is accessible to exocytic cargo, but distinct from regions containing TGN proteins (furin, VAMP4) and plasma membrane proteins (transferrin receptor) that cycle through endosomes.

The relationship between TGN and plasma membrane Sec6/8 complexes

At steady-state, membrane-bound Sec6/8 complexes are associated with both TGN (60–70%) and plasma membrane cell–cell contact sites (20–30%) in NRK-49F cells, which raises the question of whether a relationship exists between these different pools.

To investigate a possible precursor product relationship between TGN- and plasma membrane–bound Sec6/8 complexes, we relied on our ability to resolve these organelles by isopycnic centrifugation in linear iodixanol gradients (Fig. 3). NRK-49F cells were pulse-labeled with ^{35}S-methionine/cysteine, chased for times up to 2 h, homogenized, and fractionated. After detergent lysis of gradient fractions, Sec8 and P-cadherin were sequentially immunoprecipitated from each fraction. Immediately after metabolic radiolabeling, >90% of labeled P-cadherin is recovered in fractions 13–22, and thus cofractionates with marker proteins of the ER (BiP) and TGN (VAMP4/furin) (see Fig. 3 A). Less than 10% of newly synthesized P-cadherin is recovered in low density fractions containing plasma membrane markers such as syntaxin4. After 1 h chase, ~30% of labeled P-cadherin had reached plasma membrane fractions, and by 2 h chase nearly 70% was found in plasma membrane fractions (Fig. 7 A). Time-dependent increases in plasma membrane P-cadherin were balanced by concomitant decreases of P-cadherin in ER/TGN fractions and coincide with established kinetics for movement of cargo from the ER to the plasma membrane in NRK cells (Green et al., 1987).

Sec8 had very different distribution profiles at each chase time compared with those of P-cadherin (Fig. 7 B). First,

Sec8 was associated with plasma membrane immediately after the pulse, and the relative amounts of Sec8 on plasma membrane (30%) and TGN (55%) were comparable to the steady-state distribution of Sec8 between those membranes (Fig. 3 A). Second, during the chase, the relative amount of Sec8 associated with plasma membrane did not increase (27% at 1 h; 29% at 2 h), nor did the amount associated with the TGN decrease (53% at 1 h; 50% at 2 h). Instead, these two pools of metabolically labeled Sec8 were degraded at similar rates and the total pool of Sec8 turned over with a half-time of ~2 h (Fig. 7 B, inset).

To further investigate a possible relationship between TGN- and plasma membrane–associated Sec6/8 complexes, the fate of newly synthesized Sec8 was determined in cells in which vesicle trafficking from the TGN was inhibited by brefeldin A (BFA). Brief exposure of NRK cells to BFA resulted in loss of TGN membrane staining of Sec6 (Fig. 8 A). This loss of staining does not reflect dissociation of Sec6/8 complex from TGN membranes, as iodixanol gradient fractionation of membranes from BFA-treated cells still shows cofractionation of Sec6/8 complex with TGN markers (Fig. 8 B). Note that BFA treatment only slightly reduced the amount of TGN-associated Sec6/8 complex, but had no effect on the association of Sec6/8 complex with plasma membrane (compare Figs. 3 A and 8 B). We conclude that BFA treatment does not significantly reduce steady-state association of Sec6/8 complex with either the TGN or plasma membrane cell–cell contacts, but affects TGN structure to render Sec6 epitopes inaccessible for immunofluorescence microscopy.

To follow the fate of newly synthesized Sec8 when vesicle trafficking was inhibited, cells were pretreated for 30 min with BFA before metabolic labeling for 60 min in the continued presence of the drug. In BFA-treated cells, newly synthesized Sec8 was efficiently recruited onto TGN membranes, but not onto plasma membrane (Fig. 8 C). This failure to recruit newly synthesized Sec8 onto plasma membrane was accompanied by a compensatory increase in labeled Sec8 in the cytosol of BFA-treated cells (Figs. 8 C). We conclude from this experiment that Sec6/8 complex bound to the plasma membrane before BFA treatment remains bound following BFA treatment, but that vesicle trafficking is required for recruitment of Sec8 synthesized after addition of the drug.

PKD/PKCμ was recently shown to be present in exocytic compartments of the TGN and expression of a kinase-inactive mutant (PKD-K618N) caused tubulation of the Golgi complex and arrested post-Golgi trafficking of VSVG in HeLa cells (Liljedahl et al., 2001). We examined effects of PKD-K618N expression on Sec6/8 complex distribution in NRK-52E cells and MDCK cells. Expression of PKD-K618N caused extensive tubulation in HeLa cells (unpublished data), similar to results reported previously (Liljedahl et al., 2001). When GFP-PKD-K618N was transiently expressed in NRK-52E cells, the mutant kinase colocalized with Sec6 in a perinuclear region, strengthening our conclusion that Sec6/8 complex is associated with a TGN compartment involved in exocytic protein trafficking (Fig. 9). A small amount of GFP-PKD-K618N was also present in peripheral vesicular structures that did not contain Sec6. Importantly, expression of GFP-PKD-K618N in these cells caused an expansion of the TGN and led to a significant increase in the level of Sec6 associated with this organelle compared with nontransfected neighboring cells (Fig. 9). Significantly, transient overexpression of GFP-PKD-

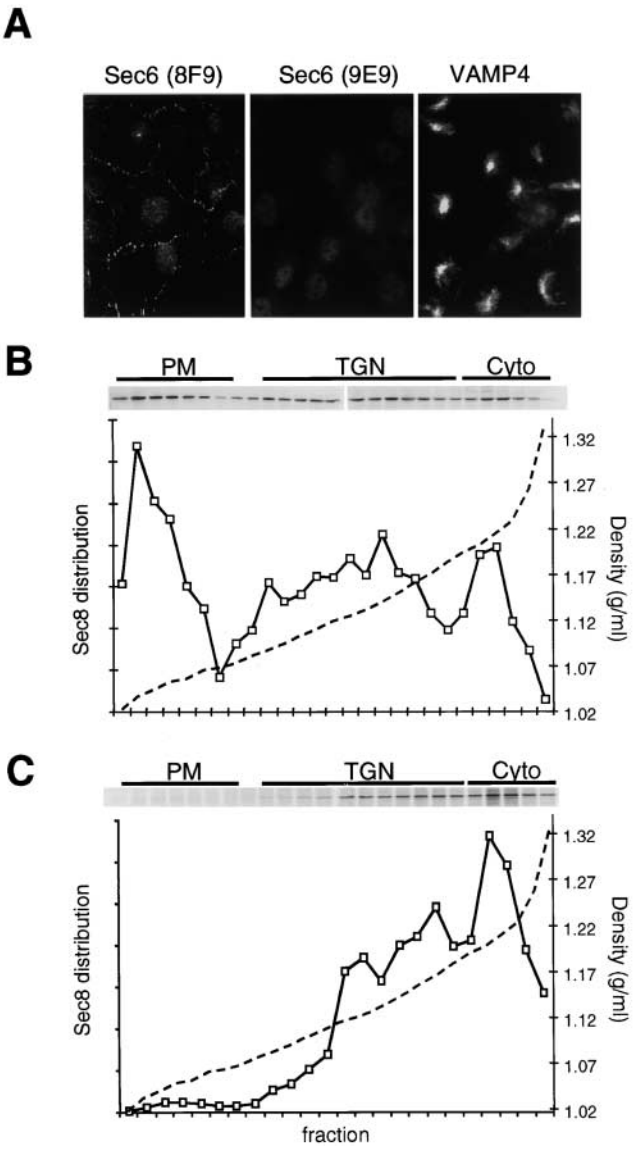

Figure 8. **Effect of BFA on steady-state binding and recruitment of newly synthesized Sec8 to plasma membrane and TGN.** (A) NRK-49F cells were incubated in 3 μg/ml BFA for 5 min, fixed, permeabilized, and stained with anti-Sec6 mAbs 8F9 or 9E9 to visualize plasma membrane and TGN Sec6/8 complexes, respectively. Cells stained with mAb 9E9 were costained with AntiVAMP4 antibodies to visualize TGN. (B) NRK-49F cells were incubated in medium containing 5 μg/ml BFA for 30 min. Cell homogenates were mixed with 10, 20, and 30% iodixanol, layered step-wise in centrifuge tubes, and centrifuged at 350,000 *g* for 3 h. Presence of Sec8 in each gradient fraction was assayed by SDS-PAGE followed by immunoblotting with specific antibodies. (C) NRK-49F cells were incubated in medium lacking methionine/cysteine and containing 5 μg/ml BFA for 30 min then metabolically labeled with ^{35}S-methionine/cysteine in the same medium for 60 min. Cell homogenates were fractionated as in B, and Sec8 was immunoprecipitated from each gradient fraction. PM, TGN, and Cyto were defined as described in the legend to Fig. 3.

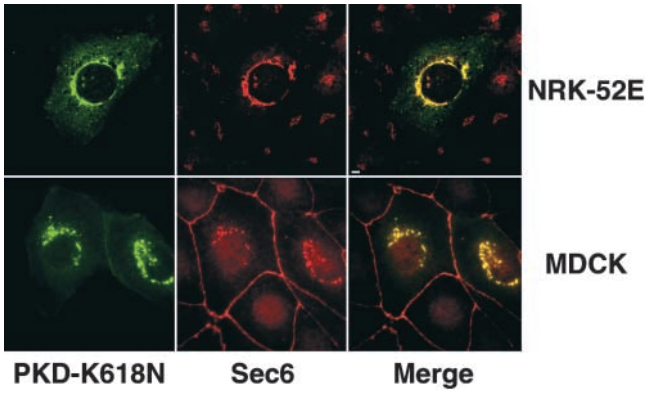

Figure 9. **Immunofluorescent staining of Sec6 in cells following transient expression of PKD-K618N.** NRK-52E and MDCK cells were transiently transfected with plasmid encoding GFP-PKD-K618N according to Materials and methods. MDCK cells were subsequently incubated at 19°C for 2 h. Cells were fixed, permeabilized, and stained for Sec6 (mAb 9H5). Bar, 5 μm.

K618N, combined with incubation of cells at 19°C for 2 h, resulted in accumulation of a pool of Sec6 in the TGN of MDCK cells (Fig. 9). Note that the low temperature incubation augmented TGN accumulation of Sec6 compared with transfected cells incubated at 37°C (unpublished data), but low temperature incubation alone was not sufficient to cause Sec6 accumulation on the TGN (Fig. 9, nontransfected cells). We conclude that although incubation of cells at 19°C slows exocytic trafficking in MDCK cells, association of Sec6/8 complex with the TGN is dependent on a process regulated by PKD, and that inactivation of this kinase is required for stable TGN binding of Sec6/8 complex in these cells.

Sec6/8 complex is required at both TGN and plasma membrane for exocytosis

Sec6/8 complex associates with TGN and plasma membrane cell–cell contacts, and there appears to be a dynamic relationship between these complexes. What is the role of Sec6/8 complexes at each site? Because monoclonal antibodies specifically bind Sec6/8 complexes associated with either TGN or plasma membrane in NRK cells, we tested these different antibodies as inhibitors of post-Golgi trafficking of ts-G-GFP in digitonin-permeabilized NRK cells. Morphological transport assays were performed using NRK-52E cells, because NRK-49F cells rounded up following permeabilization, making analysis of data impossible. Distribution of ts-G-GFP in perinuclear or peripheral regions of cells, or the region in-between these (defined generally as "cytoplasm"), was determined by quantifying total pixel intensities within boundaries defined by distributions of plasma membrane (ZO-1) or TGN (furin) markers. Representative images of individual cells (from ~15 analyses for each condition) are presented, together with histograms of data from all analyses (Fig. 10).

First, transport efficiencies in intact cells were examined as a basis for analysis of reconstituted transport in semiintact cells; we report quantitation of the data in the text. In intact NRK cells held at 19°C, ~60% of ts-G-GFP was in the perinuclear region, ~30% in the cytoplasm, and ~10% at the cell periphery. Following incubation at 32°C for 1 h, ~15% of ts-G-GFP remained in the perinuclear region, ~35% was in the cytoplasm, and ~50% was at the cell periphery. Therefore, in intact cells we observe a net transfer of ~40% of total ts-G-GFP from TGN to plasma membrane. Our definition of "cytoplasmic" ts-G-GFP is admittedly crude, and this compartment likely reflects ts-G-GFP present in at least three membrane systems: transport intermediates en route to the plasma membrane, protein inserted into plasma membrane above and below the outlined region, and protein remaining in ER/ERGIC elements outside the perinuclear region. Nevertheless, this assay allows us to observe and quantify ts-G-GFP transfer from TGN to plasma membrane.

Addition of IgG from a nonimmunized mouse to semiintact cells had no inhibitory effect on delivery of ts-G-GFP to plasma membrane (Fig. 10 A). Approximately 58% of ts-G-GFP was present at the cell periphery, where it colocalized with a plasma membrane marker (ZO-1) (Fig. 10 D). Only ~20% remained in the perinuclear region and the balance (~22%) was in the cytoplasm. Therefore, the apparent efficiency of TGN-to-plasma membrane delivery of ts-G-GFP in digitonin-permeabilized NRK-52E cells was similar to that in intact cells.

Antibodies directed against Sec6/8 epitopes exposed at the plasma membrane ("PM IgG") were tested as inhibitors of ts-G-GFP delivery to the plasma membrane (Fig. 10, B and D). Note that one of the antibodies in this group (mAb 2E9) was previously shown by us to inhibit delivery of basal-lateral low density lipoprotein receptors to the plasma membrane in MDCK cells (Grindstaff et al., 1998), so we anticipated an inhibitory effect on transport of VSV G protein (also a basal-laterally sorted protein). Quantitation of ts-G-GFP distribution in permeabilized NRK cells incubated with PM IgG shows that ~20% remains in the perinuclear region, ~35% is in the cytoplasm, and ~45% is at the cell periphery (Fig. 10 B). Although a significant amount of ts-G-GFP appeared to be trapped between TGN and plasma membrane, much of the cargo was delivered to peripheral region. However, visual inspection of peripheral regions of cells incubated with control versus PM IgG reveals differences in distribution of ts-G-GFP (Fig. 10 D). Peripheral ts-G-GFP in control cells almost always (13/15 cells examined) has a continuous, linear distribution and colocalizes with plasma membrane ZO-1 staining. In contrast, peripheral ts-G-GFP in cells incubated with PM IgG frequently (9/18 cells examined) appears discontinuous or punctate (Fig. 10 D). In other cells, peripheral ts-G-GFP has a continuous distribution that appears to be just beneath plasma membrane ZO-1 staining, distinct from control cells in which cargo and ZO-1 distributions overlap (Fig. 10 D).

When TGN Sec6 IgG cocktail was included in the transport assay, only 22% of ts-G-GFP arrived in the cell periphery and cargo was primarily (~50%) retained in the perinuclear region (Fig. 10 C). The balance of ts-G-GFP (~28%) was in cytoplasmic regions (Fig. 10 C). This latter amount is similar to control levels and indicates that TGN IgG cocktail acts to inhibit release of cargo-laden transport vesicles

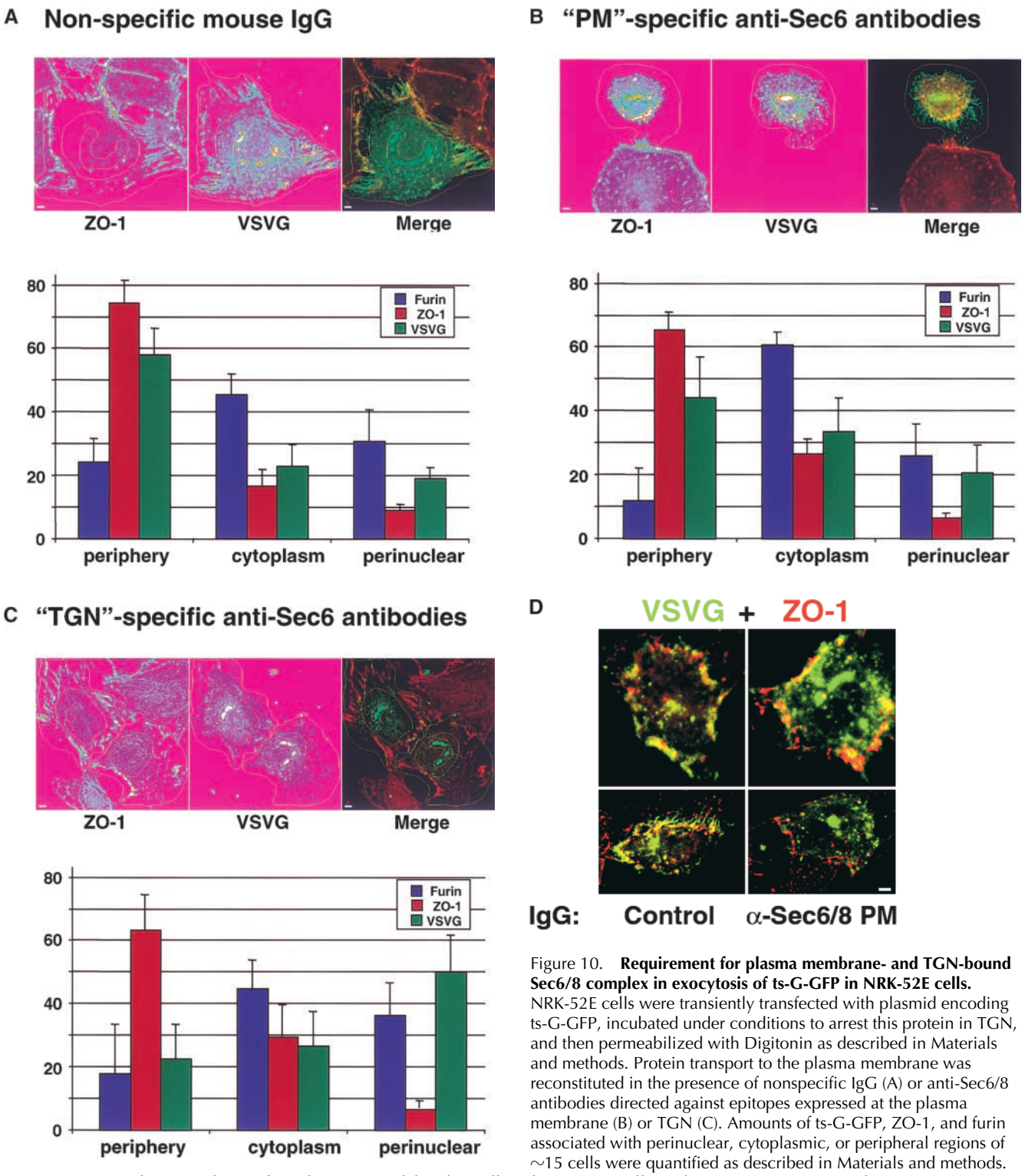

Figure 10. **Requirement for plasma membrane- and TGN-bound Sec6/8 complex in exocytosis of ts-G-GFP in NRK-52E cells.** NRK-52E cells were transiently transfected with plasmid encoding ts-G-GFP, incubated under conditions to arrest this protein in TGN, and then permeabilized with Digitonin as described in Materials and methods. Protein transport to the plasma membrane was reconstituted in the presence of nonspecific IgG (A) or anti-Sec6/8 antibodies directed against epitopes expressed at the plasma membrane (B) or TGN (C). Amounts of ts-G-GFP, ZO-1, and furin associated with perinuclear, cytoplasmic, or peripheral regions of ~15 cells were quantified as described in Materials and methods. Representative analyses are shown above histograms of data from all analyses. (D) A gallery of representative images of semiintact NRK-52E cells in which TGN to plasma membrane transport of ts-G-GFP (green) was reconstituted in the presence of either control antibodies (left) or anti-PM Sec6/8 antibodies (right) and compared with the distribution of the plasma membrane-localized ZO-1 (red). Bars, 5 μm.

from the perinuclear vicinity, rather than trafficking of these vesicles to the cell periphery. The fact that some ts-G-GFP (~12%) arrives at the cell periphery indicates that a fraction of cargo was insensitive to function-blocking antibodies or had already been packaged for post-TGN delivery before antibody addition.

Discussion

Although Sec6/8 complex associates with plasma membrane sites of exocytosis during polarized growth in budding yeast (TerBush and Novick, 1995), epithelial cells (Grindstaff et al., 1998), and neurons (Hazuka et al., 1999), this complex is expressed in many cells that do not undergo polarized membrane

growth. The results presented here show that a pool of Sec6/8 complex is localized to plasma membrane cell–cell contact sites in nonmotile fibroblasts that maintain constitutive rather than polarized plasma membrane growth. Another pool of Sec6/8 complex is located on TGN membranes that are accessible to an exocytic, but not endocytic membrane proteins. These data broaden our knowledge of the functions of the Sec6/8 complex and provide new insights into control of the exocytic pathway.

Regulation of Sec6/8 localization to TGN and plasma membrane

Previous studies indicated that the Sec6/8 complex functions at the plasma membrane (TerBush and Novick, 1995; Grindstaff et al., 1998), perhaps to tether transport vesicles during exocytosis. So our finding that a major fraction of the complex associates with the TGN in NRK-49F cells was surprising. A relationship between Sec6/8 complex pools on TGN and plasma membrane was investigated by a simple metabolic pulse-chase approach. In the presence of BFA, newly synthesized Sec6/8 complex appeared on TGN, but not plasma membrane, indicating that active exocytosis is required for recruitment of Sec6/8 complex to plasma membrane. In the absence of BFA, steady-state distribution of Sec6/8 complex between TGN and plasma membrane was reached within 30 min. This time is sufficient for arrival of some TGN-derived vesicles at the plasma membrane, but probably insufficient for steady-state to be achieved if only a TGN-derived pool of Sec6/8 complex contributed to the plasma membrane–bound pool. It is more likely that plasma membrane Sec6/8 complex is also derived from a cytosolic pool. At present, it is not known how Sec6/8 complex binds membranes. However, since Sec6/8 complex remains TGN-bound in the presence of BFA we conclude that this interaction is not controlled directly by the Sec7 family of guanine nucleotide exchange factors that are the targets of BFA action (Jackson and Casanova, 2000).

We note that two other studies were published recently that reported localization of Sec6/8 complex to a perinuclear compartment in pancreatic acinar cells (Shin et al., 2000) and PC12 cells (Vega and Hsu, 2001). However, a detailed analysis of membrane binding of Sec6/8 complex or colocalization with membrane markers was not rigorously pursued. Our finding that a pool of Sec6/8 complex associates with TGN membranes in NRK-49F cells is different from data on MDCK cells reported previously by us (Grindstaff et al., 1998). Immunofluorescent staining of polarized MDCK cells showed Sec6/8 complex almost entirely associated with plasma membrane in close proximity to tight junctions. Expression of a kinase-inactive mutant of PKD (PKD-K618N), which efficiently inhibits protein exit from TGN (Liljedahl et al., 2001), caused Sec6/8 complex to accumulate in the TGN of MDCK cells; this accumulation was augmented in PKD-K618N–expressing cells following incubation at 19°C. These data show that exocytosis in MDCK cells, as in NRK cells, is required to develop the steady-state distribution of Sec6/8 complex.

Sec6/8 functions in the exocytic pathway at the TGN and plasma membrane

A function for plasma membrane-bound Sec6/8 complex in exocytic vesicle delivery has been demonstrated genetically in yeast (Novick et al., 1981; Finger et al., 1998; Guo et al., 1999) and biochemically in mammalian cells (Grindstaff et al., 1998), but a role for Sec6/8 complex in TGN was unclear in those studies. We investigated the role of TGN-bound Sec6/8 complex in exocytosis using an antibody-blocking assay similar to that used by us previously for plasma membrane–bound Sec6/8 complex, combined with a morphological analysis of the distribution of cargo (ts-G-GFP) in late stages of the exocytic pathway. Addition of antibodies specific for the TGN Sec6/8 complex blocked ts-G-GFP transport from the perinuclear region to the cell periphery; importantly, a nonspecific antibody and antibodies specific for the plasma membrane Sec6/8 complex did not affect cargo exit from the TGN. We speculate that antibodies bound the Sec6/8 complex and sterically inhibited protein interactions normally required for cargo exocytosis, although the precise function of Sec6/8 complex on the TGN is unknown at present. It is possible that vesicles continue to bud, but cluster near the TGN because bound antibodies prevent translocation to the cell periphery. We note that cargo protein (ts-G-GFP) transits through TGN compartment that contains Sec6/8 complex, and that PKD and Sec6/8, both of which are required for cargo exit from TGN, colocalize in this TGN subcompartment. Therefore, it is tempting to speculate that this subcompartment represents a sorting domain for a class of exocytic membrane proteins. In this context, Fölsch et al. (2001) have also concluded that μ1B, which is required for sorting of the same cargo, is localized in the TGN in a subcompartment different from that of μ1A and furin.

When ts-G-GFP was released from TGN in the presence of antibodies to the plasma membrane Sec6/8 complex it accumulated in aggregates that were frequently localized adjacent to plasma membrane, but did not costain with markers of the plasma membrane. This distribution was different from that in control cells in which ts-G-GFP had a linear distribution along the plasma membrane coincident with that of ZO-1. We suggest that antibodies to the plasma membrane Sec6/8 complex sterically inhibited protein interactions required for docking of post-TGN exocytic vesicles with the plasma membrane, and as a consequence vesicles containing ts-G-GFP stacked up at these sites. This result provides a visual affirmation of our previous results in which antibodies to the plasma membrane Sec6/8 complex blocked basal-lateral plasma membrane delivery of low density lipoprotein receptor in polarized MDCK cells (Grindstaff et al., 1998). It is noteworthy that in MDCK cells VSVG protein is also delivered to the basal-lateral membrane, indicating that the Sec6/8 complex is required for delivery of vesicles containing this class of proteins in both polarized and nonpolarized cells. However, analysis of additional apically and basal-laterally targeted membrane proteins will be required to show this unequivocally.

Materials and methods

Antibodies and fluorescent probes

Mouse monoclonal antibodies against Sec6 (9E9 and 9H5) and Sec8 (2E9, 2E12, 5C3, 8F12, and 10C2) have been described previously (Hsu et al., 1996; Kee et al., 1997). Other Sec6 mAbs used (3F3, 8F9, 10C3, and 15C2) were produced at the same time as 9E9 and 9H5 (Kee et al., 1997). Affinity-purified rabbit polyclonal anti-Exo70 was generated by immunization with bacterially expressed 17.9-kD fragment of Exo70 (amino acids 503–653)

fused to glutathione *S*-transferase, and was generously provided by Dr. Patrick Brennwald (Weill Medical College, Cornell University, Ithaca, NY). Affinity-purified rabbit polyclonal antisyntaxin4 was provided by Dr. David E. James (University of Queensland, Australia) (Tellam et al., 1997). Affinity-purified rabbit polyclonal antibodies to syntaxin13 (Prekeris et al., 1998), VAMP4 (Steegmaier et al., 1999), and VAMP8 (Steegmaier et al., 2000), and mouse mAb to syntaxin13 (Prekeris et al., 1998) were provided by Dr. Richard H. Scheller (Stanford University, Stanford, CA). Rabbit polyclonal antibodies raised against α-catenin and the conserved cytoplasmic domain of cadherins (E2) have been described previously (Marrs et al., 1993; Hinck et al., 1994). Polyclonal antibodies to occludin, ZO-1, and ZO-2 were from Zymed Laboratories. Polyclonal antibodies to furin and BiP were from Affinity BioReagents, Inc. Texas red transferrin was from Molecular Probes, Inc. Plasmid encoding the temperature-sensitive mutant viral glycoprotein VSVG-tsO45 fused to GFP (ts-G-GFP) (Scales et al., 1997) was provided by Drs. Suzie J. Scales and Richard H. Scheller (Stanford University, Stanford, CA). Plasmid encoding a kinase-inactive form of PKD (pEGFP-PKD-K618N) was described previously (Liljedahl et al., 2001) and was provided by Dr. Vivek Malhotra (University of California, San Diego, CA).

Cell culture methodology

NRK-49F (ATCC CRL 1570) and NRK-52E (ATCC CRL 1571) cells were maintained in DME supplemented with 10% fetal bovine serum. In some experiments, cells were incubated for 5–30 min in 3–5 μg/ml BFA (Calbiochem), or medium containing 20 μg/ml nocodazole (Sigma-Aldrich) for 2 h (Reaves and Banting, 1992). For internalization of Texas red transferrin, cells were preincubated at 37°C in serum-free DME containing 3% BSA for 60 min, then incubated at 0°C for 60 min in the same medium supplemented with 100 μg/ml Texas red transferrin. After three washes with medium, internalization of fluorescent transferrin was initiated by addition of warm medium and incubation of cells at 37°C for different lengths of time. Transfection of NRK-49F and NRK-52E cells was performed by electroporating cells using 10 μg DNA as described previously (Chao et al., 1999). Transfection of MDCK cells was achieved using the calcium phosphate precipitation method (Ausubel et al., 1987). Cells were fixed and processed for immunofluorescent staining 48–72 h after transfection. To synchronize ts-G-GFP in different exocytic compartments, transfected cells were incubated at 40°C for 12 h to accumulate ts-G-GFP in the ER, shifted to 32°C for 7.5 min to allow ts-G-GFP to fold, and subsequently transferred to 19°C for 2 h to accumulate protein in the TGN. Trafficking of protein from the TGN to plasma membrane was initiated by shifting cultures from 19°C to 32°C.

Cell fractionation in iodixanol gradients

Cell homogenization and separation of membrane and cytosolic fractions was achieved by centrifugation in 30% (wt/vol) iodixanol (Grindstaff et al., 1998). Separation of different membrane compartments was achieved by centrifugation in three-step 10–20–30% (wt/vol) iodixanol gradients. Briefly, one-third of the postnuclear supernatant was mixed with Opti-Prep (60% (wt/vol) iodixanol (Nycomed) and homogenization buffer to generate solutions containing 10, 20, or 30% iodixanol. Equal volumes of these three solutions were layered in centrifuge tubes and samples were centrifuged at 353,000 *g* for 3 h at 4°C in a Beckman Coulter Vti65 rotor. Fractions (0.5 ml) were collected and proteins were separated by SDS-PAGE and immunoblotted (Grindstaff et al., 1998).

Immunofluorescent staining

Cells were fixed in 4% paraformaldehyde for 30 min, before or after extraction at 0°C for 10 min with 1% Triton X-100 in buffer containing 10 mM Pipes, pH 6.8, 50 mM NaCl, 300 mM sucrose, 3 mM $MgCl_2$, 0.1 mg/ml RNase, 0.1 mg/ml DNase, and protease inhibitors (CSK buffer). For immunofluorescent staining of TGN/endosomes (Figs. 4–7, 9, and 10), cells were fixed and then permeabilized with 0.075% saponin. Monoclonal Sec6 or Sec8 antibodies (as hybridoma supernatants diluted 1:4), monoclonal syntaxin13 antibody (1:1,000), and polyclonal antibodies to E/P-cadherin (1:25), α-catenin (1:500), occludin (1:500), ZO-1 (1:300), ZO-2 (1:200), VAMP4 (1:500), VAMP8 (1:100), and furin (1:100) were applied to cells for 2 h at 4°C. Fluorescein and rhodamine-conjugated secondary antibodies (Jackson ImmunoResearch Laboratories) diluted at 1:200, or rhodamine-phalloidin (1:40) were applied for 1 h at 4°C. Coverslips were washed five times and mounted in VectaShield (Vector Laboratories). Samples were viewed with either a ZEISS Axioplan microscope (100× objective) or a Molecular Dynamics MultiProbe 2010 confocal laser scanning microscope (63× objective).

Metabolic pulse-chase analysis

NRK-49F cells were incubated in methionine/cysteine-free DME for 30 min in the absence or presence of 5 μg/ml BFA. Cells were metabolically labeled with 200 μCi/ml ^{35}S-proMix (Amersham Pharmacia Biotech) for 30 min, then chased for 0, 1, 2, or 3 h in DME containing 0.2 mM methionine/cysteine. To determine the overall stability of Sec8 in NRK-49F cells, cells were extracted in CSK for 30 min at 4°C. To determine the relative amount of pulse-labeled Sec8 and P-cadherin associated with different membrane compartments during the chase, cells were homogenized at each time point and postnuclear supernatants were fractionated in linear three-step (10–20–30%) iodixanol gradients. Fractions (0.5 ml) were collected and processed for immunoprecipitation with Sec8 antibodies (5C3, 2E12, and 10C2) or a pan-cadherin rabbit polyclonal antibody (E2) (Pasdar and Nelson, 1989).

Morphological assay for plasma membrane delivery of ts-G-GFP

NRK-52E cells were transfected with plasmid encoding ts-G-GFP and protein was accumulated in the TGN as described above. Cells were permeabilized with digitonin (30 μg/ml) and incubated in transport mix containing control or anti-Sec6/8 antibodies at 19°C for 15 min, then shifted to 32°C for 60 min. Transport mix contained 10 mg/ml bovine brain cytosol, 2.5 mM MgATP, 1.25 mM GTP, 15 mM creatine phosphate, 0.25 mg/ml creatine kinase, 1 mM DTT, and protease inhibitors in buffer containing 20 mM Hepes KOH, 90 mM KOAc, 2 mM $Mg(OAc)_2$, 0.05 mM EGTA, and 0.9 mM $CaCl_2$. After incubation at 32°C for 60 min, coverslips were transferred to 0°C and processed for immunofluorescence as above. Cells were incubated with antibodies to furin (to stain TGN), ZO-1 (to stain plasma membrane), or with secondary anti–mouse antibodies (to stain control and AntiSec6/8 antibodies introduced into permeabilized cells). Serial confocal sections were collected and analyzed using ImageSpace, v. 3.2 software (Molecular Dynamics). Cell periphery, perinuclear regions, and the region in between ("cytoplasm") were manually outlined and fluorescent signals in these areas were quantified as described previously (Pepperkok et al., 1993; Hirschberg et al., 1998).

This work was supported by a grant from the National Institutes of Health to W.J. Nelson (GM35527). C. Yeaman was supported by a Walter V. and Idun Y. Berry fellowship. K.K. Grindstaff was supported by a senior postdoctoral fellowship from the American Cancer Society.

Submitted: 23 July 2001
Revised: 28 September 2001
Accepted: 1 October 2001

References

Ausubel, F.M., R. Brent, R.E. Kingston, D.D. Moore, J.G. Seidman, J.A. Smith, and K. Struhl. 1987. Current Protocols in Molecular Biology. Vol. 1. John Wiley and Sons, New York. 86–102.

Brennwald, P., B. Kearns, K. Champion, S. Keranen, V. Bankaitis, and P. Novick. 1994. Sec9 is a SNAP-25-like component of a yeast SNARE complex that may be the effector of Sec4 function in exocytosis. *Cell.* 79:245–258.

Cereijido, M., J. Valdes, L. Shoshani, and R.G. Contreras. 1998. Role of tight junctions in establishing and maintaining cell polarity. *Annu. Rev. Physiol.* 60:161–177.

Chao, D.S., J.C. Hay, S. Winnick, R. Prekeris, J. Klumperman, and R.H. Scheller. 1999. SNARE membrane trafficking dynamics in vivo. *J. Cell Biol.* 144: 869–881.

Delgrossi, M.H., L. Breuza, C. Mirre, P. Chavrier, and A. Le Bivic. 1997. Human syntaxin 3 is localized apically in human intestinal cells. *J. Cell Sci.* 110: 2207–2214.

Drubin, D.G., and W.J. Nelson. 1996. Origins of cell polarity. *Cell.* 84:335–344.

Finger, F.P., T.E. Hughes, and P. Novick. 1998. Sec3p is a spatial landmark for polarized secretion in budding yeast. *Cell.* 92:559–571.

Fölsch, H., M. Pypaert, P. Schu, and I. Mellman. 2001. Distribution and function of AP-1 clathrin adaptor complexes in polarized epithelial cells. *J. Cell Biol.* 152:595–606.

Fujita, H., P.L. Tuma, C.M. Finnegan, L. Locco, and A.L. Hubbard. 1998. Endogenous syntaxins 2, 3 and 4 exhibit distinct but overlapping patterns of expression at the hepatocyte plasma membrane. *Biochem. J.* 329:527–538.

Gaisano, H.Y., M. Ghai, P.N. Malkus, L. Sheu, A. Bouquillon, M.K. Bennett, and W.S. Trimble. 1996. Distinct cellular locations of the syntaxin family of proteins in rat pancreatic acinar cells. *Mol. Biol. Cell.* 7:2019–2027.

Garcia, E.P., P.S. McPherson, T.J. Chilcote, K. Takei, and P. De Camilli. 1995. rbSec1A and B colocalize with syntaxin 1 and SNAP-25 throughout the axon, but are not in a stable complex with syntaxin. *J. Cell Biol.* 129:105–120.

Green, S.A., K.P. Zimmer, G. Griffiths, and I. Mellman. 1987. Kinetics of intra-

cellular transport and sorting of lysosomal membrane and plasma membrane proteins. *J. Cell Biol.* 105:1227–1240.

Grindstaff, K.K., C. Yeaman, N. Anandasabapathy, S.C. Hsu, E. Rodriguez-Boulan, R.H. Scheller, and W.J. Nelson. 1998. Sec6/8 complex is recruited to cell-cell contacts and specifies transport vesicle delivery to the basal-lateral membrane in epithelial cells. *Cell.* 93:731–740.

Guo, W., A. Grant, and P. Novick. 1999. Exo84p is an exocyst protein essential for secretion. *J. Biol. Chem.* 274:23558–23564.

Hazuka, C.D., D.L. Foletti, S.C. Hsu, Y. Kee, F.W. Hopf, and R.H. Scheller. 1999. The sec6/8 complex is located at neurite outgrowth and axonal synapse- assembly domains. *J. Neurosci.* 19:1324–1334.

Hinck, L., W.J. Nelson, and J. Papkoff. 1994. Wnt-1 modulates cell-cell adhesion in mammalian cells by stabilizing beta-catenin binding to the cell adhesion protein cadherin. *J. Cell Biol.* 124:729–741.

Hirschberg, K., C.M. Miller, J. Ellenberg, J.F. Presley, E.D. Siggia, R.D. Phair, and J. Lippincott-Schwartz. 1998. Kinetic analysis of secretory protein traffic and characterization of Golgi to plasma membrane transport intermediates in living cells. *J. Cell Biol.* 143:1485–1503.

Hsu, S.C., A.E. Ting, C.D. Hazuka, S. Davanger, J.W. Kenny, Y. Kee, and R.H. Scheller. 1996. The mammalian brain rsec6/8 complex. *Neuron.* 17:1209–1219.

Ikonen, E., M. Tagaya, O. Ullrich, C. Montecucco, and K. Simons. 1995. Different requirements for NSF, SNAP, and Rab proteins in apical and basolateral transport in MDCK cells. *Cell.* 81:571–580.

Jackson, C.L., and J.E. Casanova. 2000. Turning on ARF: the Sec7 family of guanine-nucleotide-exchange factors. *Trends Cell Biol.* 10:60–67.

Jahn, R., and T.C. Südhof. 1999. Membrane fusion and exocytosis. *Annu. Rev. Biochem.* 68:863–911.

Kee, Y., J.S. Yoo, C.D. Hazuka, K.E. Peterson, S.C. Hsu, and R.H. Scheller. 1997. Subunit structure of the mammalian exocyst complex. *Proc. Natl. Acad. Sci. USA.* 94:14438–14443.

Liljedahl, M., Y. Maeda, A. Colanzi, I. Ayala, J. Van Lint, and V. Malhotra. 2001. Protein kinase D regulates the fission of cell surface destined transport carriers from the trans-Golgi network. *Cell.* 104:409–420.

Low, S.H., S.J. Chapin, T. Weimbs, L.G. Komuves, M.K. Bennett, and K.E. Mostov. 1996. Differential localization of syntaxin isoforms in polarized Madin-Darby canine kidney cells. *Mol. Biol. Cell.* 7:2007–2018.

Low, S.H., S.J. Chapin, C. Wimmer, S.W. Whiteheart, L.G. Komuves, K.E. Mostov, and T. Weimbs. 1998. The SNARE machinery is involved in apical plasma membrane trafficking in MDCK cells. *J. Cell Biol.* 141:1503–1513.

Marrs, J.A., E.W. Napolitano, E.C. Murphy, R.W. Mays, L.F. Reichardt, and W.J. Nelson. 1993. Distinguishing roles of the membrane-cytoskeleton and cadherin mediated cell-cell adhesion in generating different Na+,K(+)-ATPase distributions in polarized epithelia. *J. Cell Biol.* 123:149–164.

Mellman, I. 1996. Endocytosis and molecular sorting. *Annu. Rev. Cell Dev. Biol.* 12:575–625.

Molloy, S.S., L. Thomas, J.K. VanSlyke, P.E. Stenberg, and G. Thomas. 1994. Intracellular trafficking and activation of the furin proprotein convertase: localization to the TGN and recycling from the cell surface. *EMBO J.* 13:18–33.

Nelson, W.J., and P.J. Veshnock. 1987. Ankyrin binding to (Na+ + K+)ATPase and implications for the organization of membrane domains in polarized cells. *Nature.* 328:533–536.

Novick, P., S. Ferro, and R. Schekman. 1981. Order of events in the yeast secretory pathway. *Cell.* 25:461–469.

Pasdar, M., and W.J. Nelson. 1989. Regulation of desmosome assembly in epithelial cells: kinetics of synthesis, transport, and stabilization of desmoglein I, a major protein of the membrane core domain. *J. Cell Biol.* 109:163–177.

Pepperkok, R., J. Scheel, H. Horstmann, H.P. Hauri, G. Griffiths, and T.E. Kreis. 1993. Beta-COP is essential for biosynthetic membrane transport from the endoplasmic reticulum to the Golgi complex in vivo. *Cell.* 74:71–82.

Prekeris, R., J. Klumperman, Y.A. Chen, and R.H. Scheller. 1998. Syntaxin 13 mediates cycling of plasma membrane proteins via tubulovesicular recycling endosomes. *J. Cell Biol.* 143:957–971.

Reaves, B., and G. Banting. 1992. Perturbation of the morphology of the trans-Golgi network following Brefeldin A treatment: redistribution of a TGN-specific integral membrane protein, TGN38. *J. Cell Biol.* 116:85–94.

Scales, S.J., R. Pepperkok, and T.E. Kreis. 1997. Visualization of ER-to-Golgi transport in living cells reveals a sequential mode of action for COPII and COPI. *Cell.* 90:1137–1148.

Shin, D.M., X.-S. Zhao, W. Zeng, M. Mozhayeva, and S. Muallem. 2000. The mammalian Sec6/8 complex localizes to $Ca2^{+}$ signaling complexes and regulates their activity. *J. Cell Biol.* 150:1101–1112.

Steegmaier, M., J. Klumperman, D.L. Foletti, J.S. Yoo, and R.H. Scheller. 1999. Vesicle-associated membrane protein 4 is implicated in trans-Golgi network vesicle trafficking. *Mol. Biol. Cell.* 10:1957–1972.

Steegmaier, M., K.C. Lee, R. Prekeris, and R.H. Scheller. 2000. SNARE protein trafficking in polarized MDCK cells. *Traffic.* 1:553–560.

Tellam, J.T., S.L. Macaulay, S. McIntosh, D.R. Hewish, C.W. Ward, and D.E. James. 1997. Characterization of Munc-18c and syntaxin-4 in 3T3-L1 adipocytes. Putative role in insulin-dependent movement of GLUT-4. *J. Biol. Chem.* 272:6179–6186.

TerBush, D.R., T. Maurice, D. Roth, and P. Novick. 1996. The exocyst is a multiprotein complex required for exocytosis in *Saccharomyces cerevisiae*. *EMBO J.* 15:6483–6494.

TerBush, D.R., and P. Novick. 1995. Sec6, Sec8, and Sec15 are components of a multisubunit complex which localizes to small bud tips in *Saccharomyces cerevisiae*. *J. Cell Biol.* 130:299–312.

Vega, I.E., and S.C. Hsu. 2001. The exocyst complex associates with microtubules to mediate vesicle targeting and neurite outgrowth. *J. of Neuroscience.* 21: 3839–3848.

Vega-Salas, D.E., P.J. Salas, D. Gundersen, and E. Rodriguez-Boulan. 1987. Formation of the apical pole of epithelial (Madin-Darby canine kidney) cells: polarity of an apical protein is independent of tight junctions while segregation of a basolateral marker requires cell-cell interactions. *J. Cell Biol.* 104: 905–916.

Wong, S.H., T. Zhang, Y. Xu, V.N. Subramaniam, G. Griffiths, and W. Hong. 1998. Endobrevin, a novel synaptobrevin/VAMP-like protein preferentially associated with the early endosome. *Mol. Biol. Cell.* 9:1549–1563.

Yeaman, C., K.K. Grindstaff, and W.J. Nelson. 1999. New perspectives on mechanisms involved in generating epithelial cell polarity. *Physiol. Rev.* 79:73–98.